Bendola Publishing
Journal of Transition Metal Complexes
Vol. 1 (2018), Article ID 236055, 10 pages
doi:10.32371/jtmc/236055

Research Article

Disposal of Heavy Transition Cd^{2+} Ions from Aqueous Solution Utilizing Nanosized Flamboyant Pod (*Delonix regia*)

Laila H. Abdel-Rahman,[1] Ahmed M. Abu-Dief,[1] M. A. Abd-El Sayed,[2] and Mallak Megalea Zikry[2]

[1] *Chemistry Department, Faculty of Science, Sohag University, 82534 Sohag, Egypt*
[2] *Medicinal and Aromatic Plants Research Department, Horticulture Research Institute (HRI), Agriculture Research Center (ARC), Mourad 9, Oula, 12613 Giza, Egypt*
Address correspondence to Ahmed M. Abu-Dief, ahmed_benzoic@yahoo.com

Received 17 December 2017; Revised 23 April 2018; Accepted 25 April 2018

Abstract The absorption of toxic heavy metal by natural adsorbents from water was indicated by investigating the effect of nanosized *Delonix regia* (*D. regia*) and the chemically modified adsorbent citric acid *D. regia* (CA-*D. regia*) for removing the Cd^{2+} ions. Different techniques were employed for characterizing the adsorbent *D. regia* such as energy-dispersive X-ray (EDX) analysis, Fourier transform infrared spectroscopy (FT-IR), transmission electron microscopy (TEM), X-ray powder diffraction (XRD), and scanning electron microscopy (SEM). The effect of temperature, dosage of adsorbent, contact time, pH, and Cd^{2+} ion concentration on the adsorption process was studied. The maximum adsorption capacity of Cd^{2+} ions by *D. regia*, (q_m), was 37.2 mg.g^{-1}. The highest removal efficiency (RE) was 96.00% at pH 4.0. FT-IR peaks indicated that the main functional groups (hydroxyl and carboxylic groups) are responsible for Cd^{2+} ions binding in the adsorption. The adsorption process was endothermic and was best described by a pseudo-second-order kinetics model. The Freundlich isotherm has a better fit with the experimental data compared to the Langmuir isotherm. These results indicated that *D. regia* is an environment-friendly, available, and low cost adsorbent for adsorbing the Cd^{2+} ions.

Keywords nanosized *Delonix regia*; kinetics; removal efficiency; adsorption; thermodynamics; isotherm

1. Introduction

The high importance of wastewater treatment lies in being a source to reduce the problem of limited and scarce water resources, which is considered the most important obstacle at all that prevents the continued implementation of plans for the state's expansion. So the addition of this resource is going to maximize the benefit from the available water resources, reduce the growing gap between available water resources and the required water needs, and maintain the international water security and human health. Water bodies and wastewater are contaminated with bacteria, waste matter, and toxic heavy metals [1]. Toxic heavy metals release into the environment causes food contamination and so food safety for the human consumption is a serious worldwide public issue and is widely addressed [2]. Cd^{2+} ion is one of the most toxic heavy metals and it is responsible for causing kidney damage, bone fraction, and red blood cells damage [3]. Ion exchange, chemical precipitation, and membrane separation methods can be used for the removal of Cd^{2+} ions from water, but these methods are considered ineffective and costly [4,5]. Waste materials generated due to agricultural by-products as a whole were 320,000,000,000 kg annually [6], such as sugar cane bagasse, peat, rice husks and straws, soya bean, saw dust, walnut and seeds hull, corn cobs, banana peels and *Psidium guajava*, maize leaves, Ulmus leaves, and *Eriobotrya japonica* [7,8]. Nowadays we face solid waste disposal problem; hence there is a need to convert this waste to be a useful, economic value product for the removal of heavy metal from aqueous solution which would be useful to the environment. Treating biomass with NaOH and citric acid increases Cd^{2+} ions uptake as the carboxyl groups increase [9]. On the other hand, *Delonix regia* (*D. regia*) plant contains chemical constituents such as flavonoid, terpenoids and its glycosides, phenolics, and phytosterol which play an important role in medicine [10]. Moreover, as this plant is considered a cheap adsorbent material this increases subsequently its economic value. From this point of view, our aim of this work is to investigate the ability of nanosized *D. regia* pods powder to remove Cd^{2+} ions from aqueous solution.

2. Experimental methods

Chemicals used in this investigation were purchased from Sigma-Aldrich (St. Louis, MO, USA).

2.1. Sample collection

The *D. regia* pods were collected from Shandawil Research Station, Sohag, Egypt.

2.2. Instruments

The investigated *D. regia* pod sample was grinded to nanosize using Retsch Muhle Brinkmann Spectro Mill MS Microgrinding Mixing Pulverizer. The structure of investigated plant was characterized by X-ray powder diffraction (XRPD), with X-ray patterns from 5° to 80° at 2θ collected by a Philips X'Pert PRO-MPD (PANalytical, The Netherlands) using graphite-monochromatized Cu K_α radiation ($\lambda = 1.54184$ Å) operating at 45 kV and 40 mA. The morphology of samples was studied by field-emission scanning electron microscopy (FE-SEM) and was performed on a JSM-6100 microscope (JEOL, Japan) with an acceleration voltage of 30 kV. The chemical composition of the synthesized nanostructures was also analyzed using energy dispersive analysis of X-ray (EDAX) unit attached with the FE-SEM. Transmission electron microscopy (TEM) images were obtained with a 2000 EX(II) microscope (JEOL, Japan) at an acceleration voltage of 200 kV. Particle-size distribution of the studied nanosized *D. regia* pod was evaluated using imageJ Launcher, broken-symmetry software, version (1.4.3.6.7) [11, 12, 13]. Hettich Centrifuge EBA 20 (D-78532 Tuttlingen) was used to centrifuge the sample after the adsorption process. The concentration of Cd^{2+} was determined using Flame Atomic Absorption Spectrometer (Flame AAS; Perkin-Elmer model; Analyst 200). AD1000 and AD1020 pH/mV/ISE/temperature bench meters were used to adjust pH of the prepared solutions. The shaking was carried out in a thermostated electronic shaker bath, Heidolph MR 3001, and centrifugation was performed on a Hettich EBA 20 centrifuge. Fourier transform infrared spectroscopy (FTIR-2000, Perkin-Elmer) was used for detection of the surface functional groups on the prepared biosorbents.

2.3. Sample pretreatment

Pods of *D. regia* were washed with water, dried, grinded, and sieved to obtain a very fine powder less than 100 nm.

2.3.1. Treatment of D. regia *by citric acid*

Chemical modification of nanosized *D. regia* powder was performed using NaOH followed by citric acid treatment [14].

2.4. Preparation of aqueous solution

Stock solution of Cd^{2+} ions was prepared by weighing out 2.726 g of $Cd(NO_3)_2 \cdot 4\,H_2O$ and dissolving it in a 1,000 mL volumetric flask; the result concentration was 1,000 mg/L.

2.5. Adsorption experiments

2.5.1. Initial Cd^{2+} ions concentration

The amount of 50 mL of Cd^{2+} ions solution of different concentrations was added to 0.3 g of the adsorbent in a bottle.

2.5.2. pH values

Experiments were carried out at different pH values (2–10) and pH was adjusted by using 0.1 M NaOH or 0.1 M HCl.

2.5.3. Adsorbent dosage

In each experiment, 50 mL of Cd^{2+} ions solution of concentration (20 mg/L) were added to different dosages of the adsorbent in a bottle.

2.5.4. Contact time

In the adsorption kinetics experiment, 0.2 L of Cd^{2+} ions solution of different concentrations were added to 1.2 g of the adsorbent in a flat bottle and then the mixture was stirred on a shaker and a contact time 20 min–120 min with time interval 20 min.

2.5.5. Adsorption isotherm

The Cd^{2+} ions distribution between the solid and liquid phases can be described by the Freundlich and Langmuir isotherms. The amount of Cd^{2+} ions adsorbed at equilibrium (q_e) increased with the initial concentration of Cd^{2+} ions, as expected [15, 16, 17, 18]. The amount of q_m is 15.26 mg/g of *D. regia*. Langmuir isotherm equation is represented in a linear form [16, 17, 18] as follows:

$$\frac{C_e}{q_e} = \frac{1}{q_m b} + \frac{C_e}{q_m}. \tag{1}$$

Plot of C_e/q_e against C_e gives a line with intercept $1/q_m b$ and slope $1/q_m$ is obtained, which shows Cd^{2+} ions adsorption isotherms of Langmuir. From the intercept and slope, the Langmuir parameters (b and q_m) are calculated [16, 17, 18]. The Freundlich equation has the general form [16, 17, 18, 19]

$$\log q_e = \log K_f + \frac{1}{n} \log C_e. \tag{2}$$

From a plot, a line with slope and intercept, $1/n$ and $\log K_f$, respectively, can be calculated. The slope, $1/n$, indicates the intensity of adsorption and $\log K_f$ indicates the adsorption capacity [20]. A dimensionless constant separator factor (R_L) can classify the isotherms [21] stated as

$$R_\mathrm{L} = \frac{1}{\left(1 + bC_o\right)}. \tag{3}$$

2.5.6. Temperature

An amount of 50 mL of different concentrations of Cd^{2+} ions solution was added to 0.3 g of the adsorbent in a bottle at different temperatures and then the mixture was stirred for 60 min on a shaker at 300 rpm. Then, it was centrifuged and the concentration of Cd^{2+} ions was determined. The relationships (1) and (2) [21] can be used to calculate $\Delta S°$,

$\Delta H°$, and $\Delta G°$ (the thermodynamic parameters for the adsorption process) [22,23,24] as follows:

$$\ln b = \frac{\Delta S°}{R} - \frac{\Delta H°}{RT}, \tag{4}$$

$$\Delta G° = \Delta H° - T\Delta S°. \tag{5}$$

2.5.7. *Calculation of Cd^{2+} ions absorption capacity (q_e)*

The amount of q_e was calculated by

$$q_e = \frac{v(C_o - C_e)}{w}. \tag{6}$$

The RE of the Cd^{2+} ions was determined using

$$\text{RE}\% = \frac{(C_o - C_e)}{C_o} \times 100, \tag{7}$$

where RE% is the percentage of the removed Cd^{2+} ions.

2.5.8. *Kinetics study*

The mechanism of the adsorption of Cd^{2+} ions was tested using pseudo-first-order [25] and pseudo-second-order kinetic models displayed by the following equations, respectively [26,27]:

$$\ln\left(q_e - q_t\right) = \ln q_e - k_1 t, \tag{8}$$

$$\left(\frac{t}{q_t}\right) = \frac{1}{k_2 q_e^2} + \left(\frac{t}{q_e}\right). \tag{9}$$

Both models are tested for suitability using correlation coefficient R^2 [26,28].

2.5.9. *Chemical treatment of the adsorbent*

An amount of 50 mL of Cd^{2+} ions solution of initial concentration 20 mg/L was added to 300 mg of a chemically treated adsorbent citric acid *D. regia* (CA-*D. regia*); the mixture was stirred for 60 min. After each experiment, the mixture was centrifuged and the concentration of each was determined using the Flame AAS.

3. Results and discussion

3.1. Characteristics of the adsorbent

3.1.1. *FT-IR analysis of the adsorbent*

An FT-IR analysis of *D. regia* and Cd^{2+} ions loaded *D. regia* (Cd-*D. regia*) (Figure 1(a)) was carried out. The FT-IR spectrum of *D. regia* indicates the functional groups. The peak appears in the region of 1,000 cm^{-1}–1,200 cm^{-1}, which is characteristic of cellulose [29]. A strong peak at 3,298 cm^{-1} was attributed to N−H bond. The shift in the peak position to 3,332 cm^{-1} in the spectrum of the Cd-*D. regia* indicates the binding of Cd^{2+} ions with amino and hydroxyl groups [30,31,32]. The peak at 2,917 cm^{-1} was assigned to CH stretching vibrations. A peak at 1,036 cm^{-1} indicated the C−O of alcohols and the shift to 1,040 cm^{-1} indicated a binding of Cd^{2+} ions with C−O group [30, 31,32,33]. A peak was observed at 1,738 cm^{-1}, which is characteristic of carbonyl group and is shifted to a wave number of 1,731 cm^{-1} on Cd^{2+} adsorption [34,35]. A peak at 1,243 cm^{-1} indicates the presence of carboxylic acids which shifted to a wave number of 1,229 cm^{-1} after Cd^{2+} ions absorption [36].

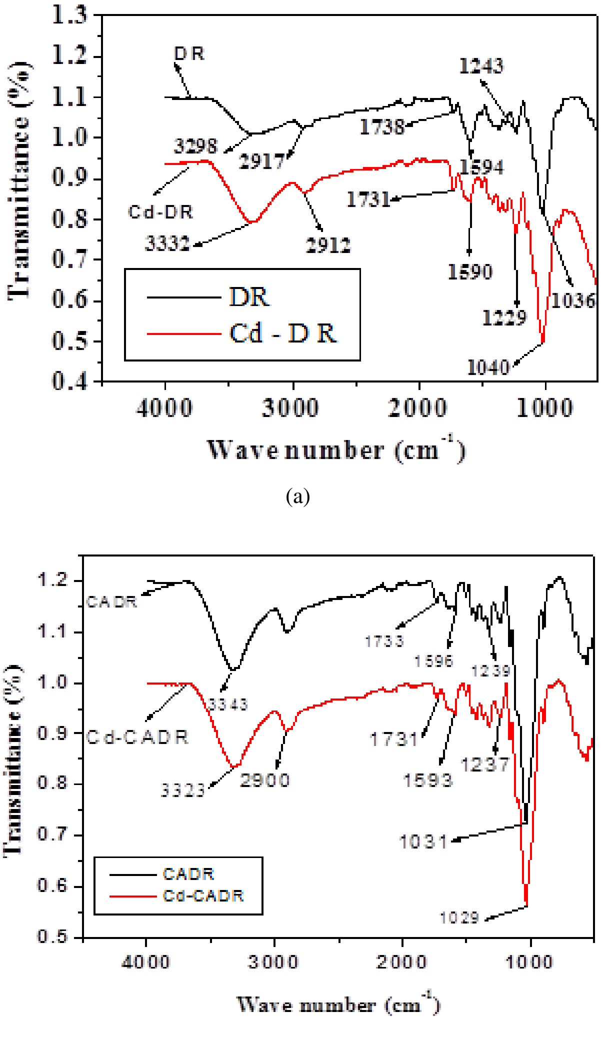

(a)

(b)

Figure 1: (a) FT-IR spectral analysis of the adsorbent *D. regia* and Cd-*D. regia*. (b) FT-IR spectral analysis of CA-*D. regia* and Cd-CA-*D. regia*.

Also, an FT-IR analysis for detecting the functional groups of CA-*D. regia* and Cd^{2+} loaded CA-*D. regia* (Cd-CA-*D. regia*) is shown in Figure 1(b). A comparison of the IR spectra of the samples of *D. regia* and CA-*D. regia* revealed that a characteristic vibration absorption band of carboxyl group at 1,733 cm^{-1} is present in the IR spectrum of CA-*D. regia* samples. This indicates the esterification between alcohol groups of cellulose in *D. regia* and citric acid. The peak at 1,733 cm^{-1} shifted to

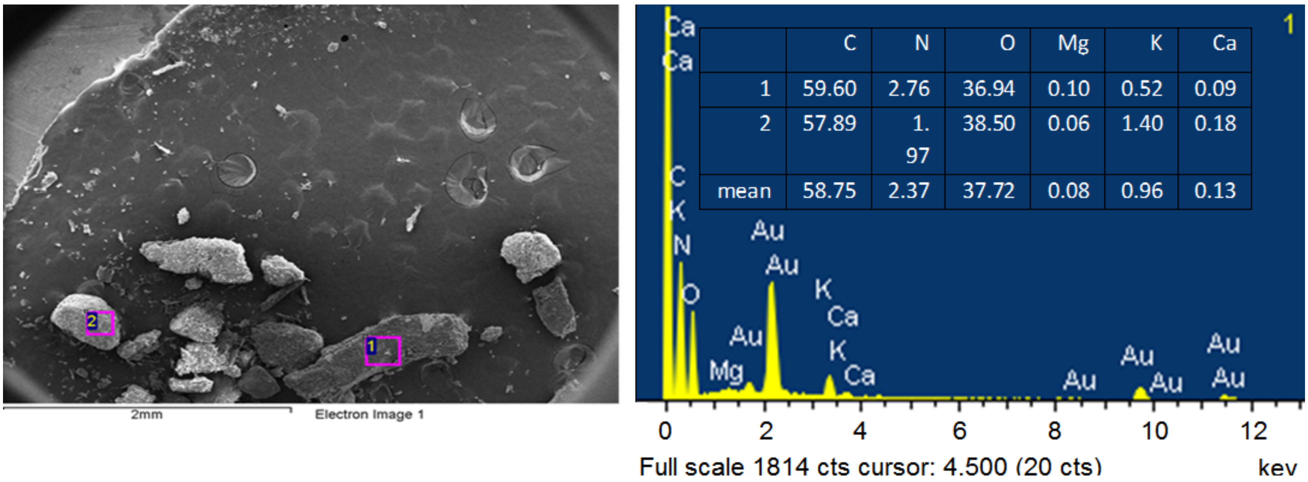

	C	N	O	Mg	K	Ca
1	59.60	2.76	36.94	0.10	0.52	0.09
2	57.89	1.97	38.50	0.06	1.40	0.18
mean	58.75	2.37	37.72	0.08	0.96	0.13

Figure 2: EDX spectrum of the investigated nanosized *D. regia* plant.

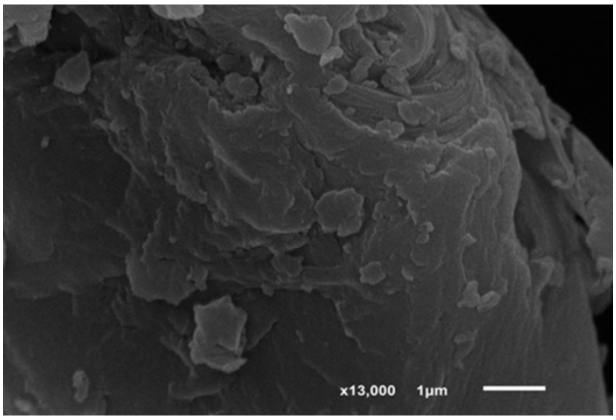

Figure 3: SEM of the adsorbent *D. regia* pod.

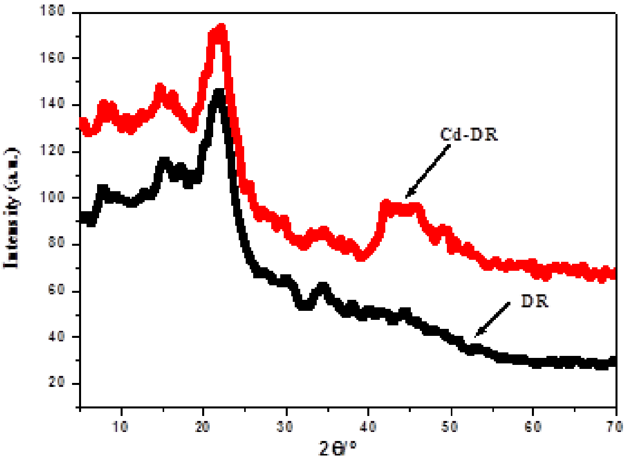

Figure 4: XRD patterns of the adsorbent *D. regia* and Cd-*D. regia*.

1,731 cm^{-1} in the spectrum of Cd-CA-*D. regia* indicating the adsorption of Cd^{2+} ions on carboxylic group. The peak around 2,550 cm^{-1} to 3,550 cm^{-1} centered at 3,343 indicates the existence of carboxylic OH groups and COOH group after CA treatment. It appears from Figure 1(b) that the different functional groups on CA-*D. regia* are responsible for the adsorption of Cd^{2+} ions. A change in peaks' position at 3,323 cm^{-1} in the spectrum of Cd-CA-*D. regia* indicates the adsorption of these Cd^{2+} ions on hydroxyl groups [14].

3.1.2. EDX analysis

To determine the composition of the investigated plant, EDX elemental analysis of *D. regia* is shown in Figure 2.

3.1.3. SEM analysis

An SEM analysis of the adsorbent *D. regia* (Figure 3) is used to show the morphology. The surface morphology of powder showed that the powder is composed of fine particles.

3.1.4. XRD analysis

XRD patterns of the *D. regia* powder (shown in Figure 4) indicate the presence of a significant amount of amorphous material due to lignin in the sample and show that the structure of *D. regia* has a different change at the appearance of amorphous peak at $2\theta = 42.16°$ after the adsorption of Cd^{2+} ions.

3.1.5. TEM analysis

The adsorbent was subjected to a TEM analysis (cf. Figure 5(a)) to examine the particle size. Figure 5(b) shows the diameter distribution histogram of the nanosized adsorbent estimated by public image analysis product (ImageJ, NIH, USA) and the size of the majority of particles was found to be 18 nm. The small size of the studied adsorbent allows it to be more efficient in the adsorption of cadmium ions.

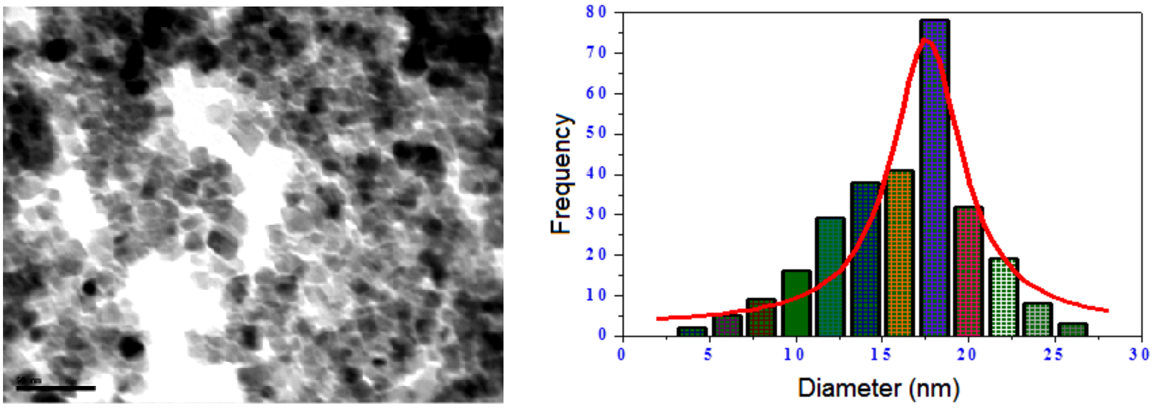

(a)

(b)

Figure 5: (a) TEM image of nanosized adsorbent *D. regia*. (b) Calculated histogram for particle size distribution of *D. regia*.

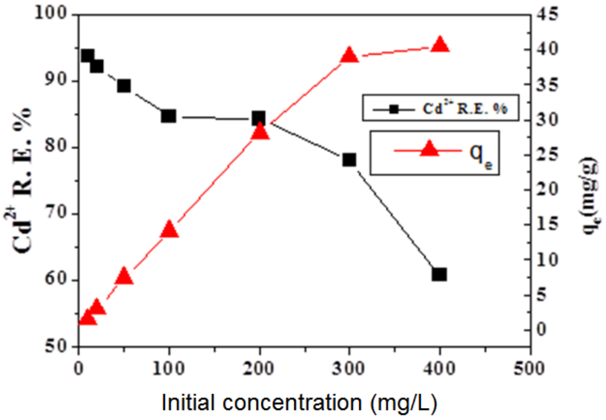

Figure 6: Effect of initial Cd^{2+} ions concentration on Cd^{2+} ions RE and q_e by *D. regia*.

Table 1: Cd^{2+} ions RE and q_e at different initial concentrations.

C_o (mg/L)	C_e (mg/L) ±SD[a]	Cd^{2+} ions RE% ±SD	q_e (mg/g) ±SD
10	0.64 ± 0.04	93.57 ± 0.04	1.56 ± 0.05
20	1.52 ± 0.10	92.42 ± 0.16	3.80 ± 0.06
50	4.46 ± 0.22	91.08 ± 0.22	7.59 ± 0.09
100	9.60 ± 0.15	90.39 ± 0.09	15.10 ± 0.08
200	23.01 ± 0.60	88.49 ± 0.06	29.50 ± 0.01
300	78.51 ± 0.70	73.75 ± 0.21	36.88 ± 0.03
400	176.64 ± 0.97	55.84 ± 0.27	37.23 ± 0.20

[a] SD = standard deviation.

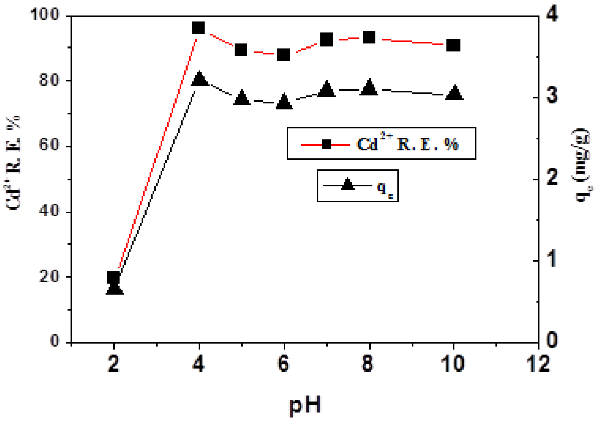

Figure 7: Effect of pH on Cd^{2+} ions RE and q_e at different pH values by *D. regia*.

Table 2: Cd^{2+} ions RE and q_e at initial concentration of Cd^{2+} (20 mg/L) and different pH values by *D. regia*.

pH	C_e (mg/L) ±SD	Cd^{2+} ions RE% ±SD	q_e (mg/g) ±SD
2	16.69 ± 0.09	19.50 ± 0.12	0.65 ± 0.02
4	0.80 ± 0.01	96.00 ± 0.06	3.20 ± 0.13
5	2.14 ± 0.02	89.29 ± 0.14	2.98 ± 0.09
6	2.42 ± 0.05	87.88 ± 0.06	2.93 ± 0.04
7	1.51 ± 0.02	92.41 ± 0.15	3.08 ± 0.08
8	1.17 ± 0.03	93.10 ± 0.13	3.10 ± 0.09
10	1.82 ± 0.04	90.88 ± 0.19	3.03 ± 0.05

3.1.6. Effect of initial concentration

Table 1 and Figure 6 illustrate the effect of Cd^{2+} ions concentration on the adsorption. The Cd^{2+} ions q_e increases as the concentration rises, as Cd^{2+} ions are more available for interaction with the adsorbent. The Cd^{2+} ions RE for initial concentration 10 mg/L is 93.57% and decreases as the concentration increases. At low concentrations of Cd^{2+} ions, a greater chance was available for metal removal as adsorption sites took up the available Cd^{2+} ions with increasing concentrations [37,38,39,40].

3.1.7. Effect of pH

Table 2 and Figure 7 illustrate the effect of pH on the adsorption process. The Cd^{2+} ions RE and q_e increase as the pH value increases. The amount of Cd^{2+} ions removed

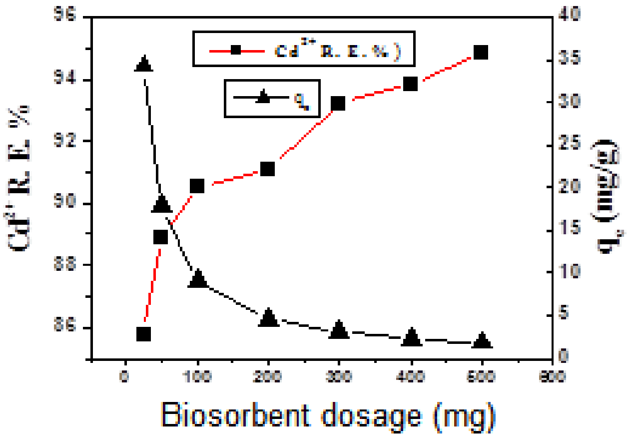

Figure 8: Effect of adsorbent dosage on Cd^{2+} ions RE and q_e by *D. regia*.

Table 3: Cd^{2+} ions RE and q_e at different adsorbent dosages by *D. regia*.

Adsorbent dosage (mg)	C_e (mg/L) ±SD	Cd^{2+} ions RE% ±SD	q_e (mg/g) ±SD
25	2.84 ± 0.08	85.79 ± 0.09	34.32 ± 0.16
50	2.22 ± 0.06	88.90 ± 0.31	17.98 ± 0.17
100	1.88 ± 0.03	90.54 ± 0.22	9.05 ± 0.10
200	1.77 ± 0.01	91.10 ± 0.31	4.56 ± 0.09
300	1.36 ± 0.03	93.21 ± 0.17	3.11 ± 0.06
400	1.24 ± 0.02	93.80 ± 0.07	2.35 ± 0.05
500	1.04 ± 0.01	94.82 ± 0.05	1.90 ± 0.01

by the *D. regia* at low pH 2 was low (0.65 mg/g) with RE of 19.5% compared to the amounts removed at pH 4 to pH 10 which ranged from 3.2 mg/g (RE 96%) at pH 4 to 2.98 mg/g (RE 89.29%) at pH 5. This is because at low pH value the concentration of H^+ is high [33], as H^+ ions were being removed by the adsorbent instead of the Cd^{2+} ions [34, 41]. At a higher concentration of H^+ ions, the adsorbent surface becomes positive charge thus reducing the attraction between *D. regia* and Cd^{2+} ions [42].

3.1.8. Effect of the adsorbent dosage

Table 3 and Figure 8 illustrate the effect of the adsorbent dosage. RE increases with the lowest value of 85.79% and the highest value of 94.82% obtained with 25 mg and 500 mg of the adsorbent, respectively. This is because at high dosage, there is an increase in surface area and availability of adsorption sites, but q_e decreases with a decrease in the amount of Cd^{2+} ions adsorbed per unit weight of adsorbent [43,44,45].

3.1.9. Effect of contact time

Figure 9 and Table 4 illustrate the effect of contact time on the adsorption of Cd^{2+} ions by *D. regia*. The amount of Cd^{2+} ions absorbed increased with an increase in the contact time and reached equilibrium in 60 min. This is because a long contact time and availability of active sites was followed by a reduction in the Cd^{2+} ion uptake. The removal of Cd^{2+} ions remains constant as the active sites are less available [46, 47].

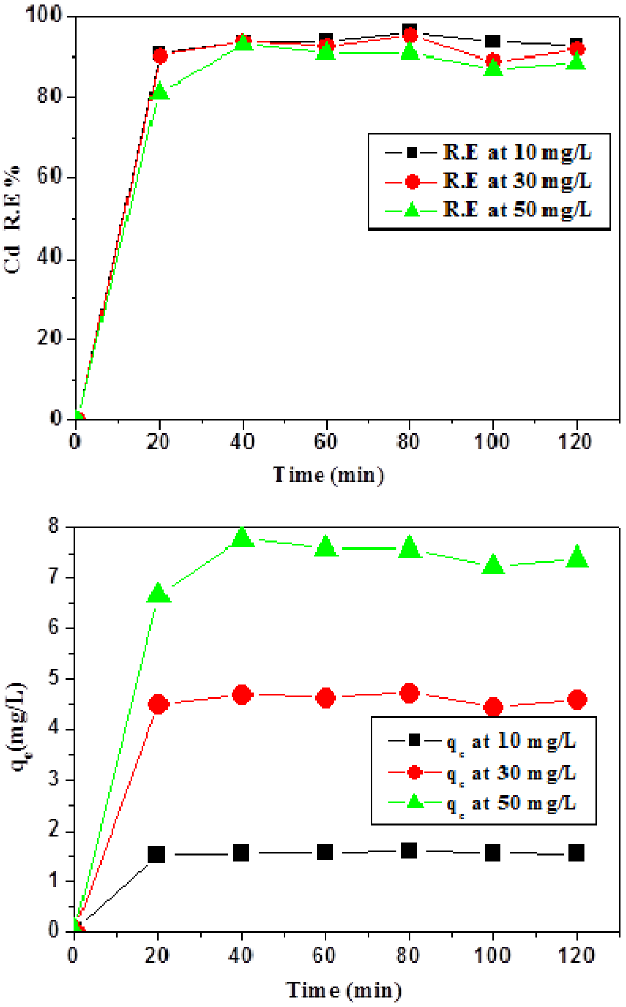

Figure 9: Effect of contact time on Cd^{2+} ions RE and q_e at different initial concentrations (10 mg/L, 30 mg/L, and 50 mg/L) by *D. regia* pod.

3.1.10. Effect of temperature

Table 5 and Figure 10 illustrate the effect of temperature on the adsorption. The Cd^{2+} ions RE and q_e by *D. regia* increase while the temperature is increasing, as the active sites have increased and encouraged the process of adsorption, due to an increase in the movement of the Cd^{2+} ions and pore size indicating an endothermic process [48,49].

3.1.11. Adsorption isotherm

Parameters of Cd^{2+} ions adsorption are given in Table 6. A dimensionless constant separator factor (R_L) can classify

Table 4: Effect of contact time on Cd^{2+} ions RE and q_e at different initial concentrations (10 mg/L, 30 mg/L, and 50 mg/L) by *D. regia*.

Time (min)	Cd^{2+} RE% at C_o (10)	Cd^{2+} RE% at C_o (30)	Cd^{2+} RE% at C_o (50)	q_t at C_o (10)	q_t at C_o (30)	q_t at C_o (50)	C_t at C_o (10)	C_t at C_o (30)	C_t at C_o (50)
20	90.97	90.20	80.99	1.52	4.51	6.67	0.90	2.93	10.00
40	93.57	94.07	93.16	1.56	4.70	7.76	0.64	1.78	3.42
60	93.98	92.80	91.08	1.57	4.64	7.59	0.60	2.16	4.46
80	96.29	95.40	90.87	1.61	4.73	7.57	0.37	1.37	4.56
100	93.88	88.92	86.86	1.56	4.45	7.24	0.61	3.32	6.57
120	92.95	91.86	88.55	1.55	4.58	7.38	0.70	2.50	5.73

Table 5: Effect of temperature on Cd^{2+} RE and q_e by *D. regia*.

Temperature (°C)	Cd^{2+} RE% at C_o (10)	Cd^{2+} RE% at C_o (30)	Cd^{2+} RE% at C_o (50)	q_t at C_o (10)	q_t at C_o (30)	q_t at C_o (50)	C_t at C_o (10)	C_t at C_o (30)	C_t at C_o (50)
25	93.57	92.42	91.08	1.56	3.08	7.59	0.64	1.52	4.46
30	93.93	93.21	92.63	1.57	3.11	7.72	0.61	1.36	3.68
40	95.88	93.81	93.69	1.60	3.13	7.81	0.41	1.24	3.15
50	94.69	92.03	92.48	1.58	3.07	7.71	0.53	1.59	3.76

Table 6: Isotherm constants of Cd^{2+} ions adsorption at various temperatures.

T(K)	Langmuir			Freundlich			
	q_m(mg/g) ±SD	b(L/mg) ±SD	R_2	n ±SD	$1/n$	K_f (mg/g) ±SD	R_2
298	23.49 ± 0.12	0.11 ± 0.03	0.94	1.22 ± 0.09	0.81	2.22 ± 0.15	0.99
303	38.63 ± 0.15	0.07 ± 0.01	0.88	1.13 ± 0.05	0.88	2.41 ± 0.08	0.99
313	22.34 ± 0.11	0.16 ± 0.06	0.59	1.29 ± 0.07	0.77	3.00 ± 0.14	0.98
323	26.42 ± 0.19	0.10 ± 0.06	0.40	1.25 ± 0.06	0.80	2.46 ± 0.31	0.97

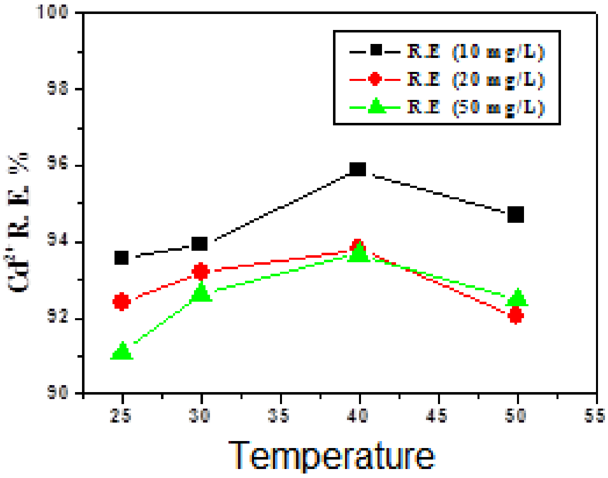

Figure 10: Effect of temperature on Cd^{2+} ions RE by *D. regia*.

the isotherms [50] stated in (3). R_L values have arranged from 0.1114 to 0.5979 (Table 7). The n values were greater than 1 [51], indicating a formation of a bond between Cd^{2+} ions and the adsorbent and also a favorable adsorption (i.e., Cd^{2+} ions adsorption on *D. regia* is favorable). According to linearity coefficients ($R^2 = 0.999$), Freundlich model has a good fit to the adsorption of Cd^{2+} ions on *D. regia* (Figures 11 and 12).

Table 7: A dimensionless constant separator factor (R_L) for Langmuir type adsorption process.

C_o (mg/L)	R_L at 25°C	R_L at 30°C	R_L at 40°C	R_L at 50°C
10	0.49	0.60	0.39	0.50
20	0.32	0.43	0.24	0.33
50	0.16	0.23	0.11	0.17

Table 8: Thermodynamic parameters for the adsorption process.

Temperature (K)	$\Delta G°$ (KJ/mol)	$\Delta H°$ (KJ/mol)	$\Delta S°$ (J/mol K)
298	6.19	27.50	71.51
303	5.83		
313	5.12		
323	5.01		

3.1.12. Thermodynamic studies

From a plot $\ln b$ against 1/T, thermodynamic parameters were obtained. The Cd^{2+} ions q_e by *D. regia* increased as temperature increased, indicating that the adsorption process was endothermic. Thermodynamic parameters ($\Delta G°$, $\Delta S°$, and $\Delta H°$) (Table 8) were determined using (1) and (2) [52]. The adsorption process of Cd^{2+} ions on the *D. regia* was endothermic as $\Delta H°$ values were positive. A positive $\Delta G°$ value suggested an ion-exchange mechanism [53]. The more positive value of $\Delta S°$, the more randomness there is during the adsorption process [25, 54].

Table 9: Kinetic parameters of Cd^{2+} ions adsorption onto *D. regia*.

C_o (mg/L)	Pseudo-first-order kinetics			Pseudo-second-order kinetics			Observed q_e (mg/g) ±SD
	k_1 (1/min) ±SD	q_e(mg/g) ±SD	R^2	k_2 (g/mg.min) ±SD	q_e(mg/g) ±SD	R^2	
10	0.12 ± 0.01	0.99 ± 0.03	0.98	0.97 ± 0.04	1.60 ± 0.06	0.999	1.57 ± 0.05
30	0.08 ± 0.003	1.65 ± 0.05	0.61	0.49 ± 0.02	4.73 ± 0.04	0.999	4.71 ± 0.04
50	0.14 ± 0.02	13.37 ± 0.09	0.93	0.14 ± 0.01	7.69 ± 0.08	0.998	7.59 ± 0.09

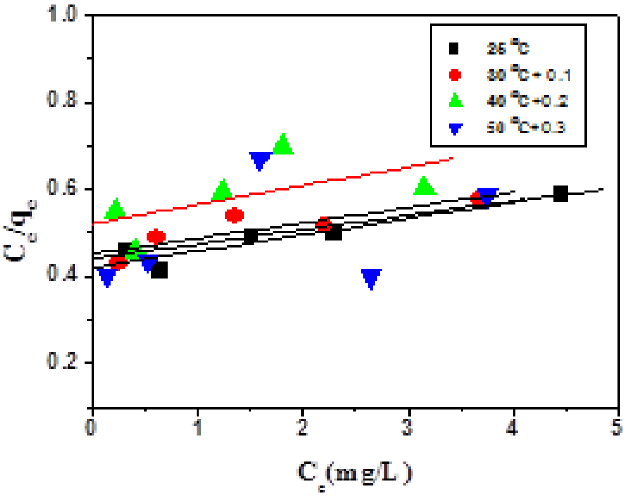

Figure 11: Linearized adsorption isotherms of Langmuir.

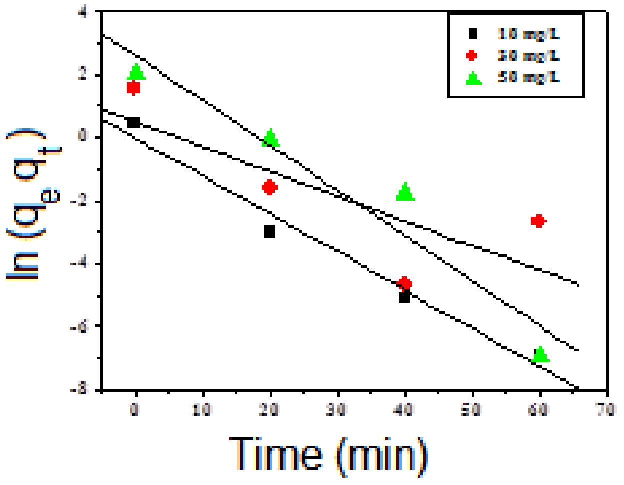

Figure 13: Pseudo-first-order kinetics for the adsorption of Cd^{2+} ions by *D. regia*.

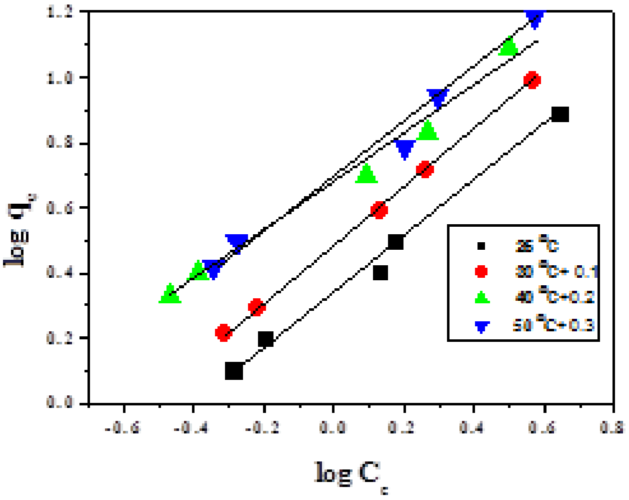

Figure 12: Linearized adsorption isotherms of Freundlich.

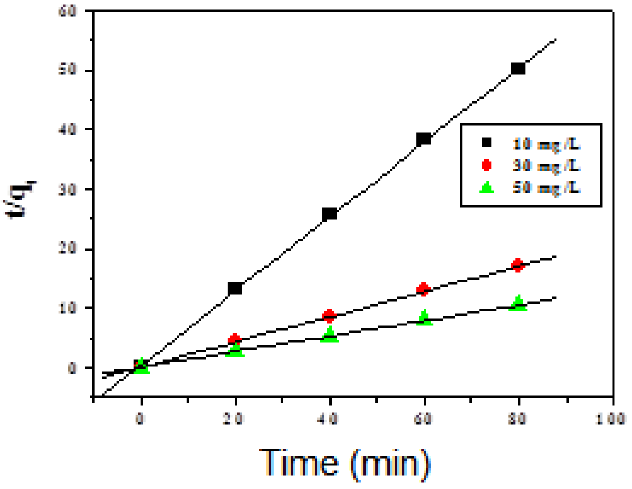

Figure 14: Pseudo-second-order kinetics for the adsorption of Cd^{2+} ions by *D. regia*.

3.1.13. Kinetic studies

Pseudo-first-order and pseudo-second-order kinetics can be used to test the mechanism of the adsorption of metal ions [28,29]. The adsorption kinetic of the adsorbed Cd^{2+} ions was studied (Figures 13 and 14). The pseudo-first-order model is not good in studying the kinetics of the adsorption of Cd^{2+} ions compared to pseudo-second-order model ($R^2 = 0.999$) for Cd^{2+} ions (Table 9) [28]. So the second-order kinetics is good in studying the kinetics of the adsorption of Cd^{2+} ions, as the calculated q_e (7.69 mg/g) is very close to the experimental q_e (7.59 mg/g), suggesting that the adsorption solutions involve the Cd^{2+} ion and the adsorbent [51,52].

Table 10: Effect of chemical treatment of the adsorbent on the adsorption efficiency.

Adsorbent	*D. regia*			
C_o (20 mg/L) of metal ions	*D. regia*		CA-*D. regia*	
	C_e (mg/L) ±SD	RE% ±SD	C_e (mg/L) ±SD	RE% ±SD
Cd^{2+}	1.52 ± 0.02	92.42 ± 0.19	0.259 ± 0.03	98.71 ± 0.15

3.1.14. Effect of chemical treatment of the adsorbent on the adsorption efficiency

The effect of chemical treatment of the adsorbent *D. regia* by esterifying with NaOH followed by citric acid treatment (CA-*D. regia*) on the RE compared with *D. regia* was studied and shown in Table 10. It was observed that the RE percentage of metal ions by CA-*D. regia* was higher than that of Cd^{2+} ions by *D. regia*, as the chemical treatment of *D. regia* with NaOH and citric acid increases Cd^{2+} ions adsorption as the carboxyl group of the biomass increases [14,43,55].

4. Conclusion

Nanosized flamboyant pod *D. regia* was used for the adsorption of Cd^{2+} from aqueous solution. The investigated biosorbent was characterized by using FT-IR, SEM, TEM, XRD, and EDX techniques. The adsorption process depends on temperature, pH, contact time, dosage, and Cd^{2+} ions concentration.

Adsorption of Cd^{2+} ions from solution obeyed the Freundlich isotherm model. The q_m of Cd^{2+} ions on *D. regia* is $37.2\,mg.g^{-1}$. The adsorption process was endothermic having an ion exchange mechanism. Second-order kinetics models are better in studying the kinetics of adsorption. The results showed that *D. regia* pod biosorbent proved to be a very effective biosorbent in the removal of Cd^{2+} ions from water.

Acknowledgments The authors thank both Oviedo University, Spain and Sohag University, Egypt for financial support.

Conflict of interest The authors declare that they have no conflict of interest.

References

[1] R. H. Vieira and B. Volesky, *Biosorption: a solution to pollution?*, Int Microbiol, 3 (2000), 17–24.

[2] A. M. Abu-Dief and S. K. Hamdan, *Functionalization of magnetic nano particles: synthesis, characterization and their application in water purification*, Am J Nanosci, 2 (2016), 26–40.

[3] G. A. Drasch, *An increase of cadmium body burden for this century—An investigation on human tissues*, Sci Total Environ, 26 (1983), 111–119.

[4] E. N. Ali, S. R. Alfarra, M. M. Yusoff, and M. L. Rahman, *Environmentally friendly biosorbent from Moringa oleifera leaves for water treatment*, Int J Environ Sci Dev, 6 (2015), 165–169.

[5] K. Kelly-Vargas, M. Cerro-Lopez, S. Reyna-Tellez, E. R. Bandala, and J. L. Sanchez-Salas, *Biosorption of heavy metals in polluted water, using different waste fruit cortex*, Phys Chem Earth, 37 (2012), 26–29.

[6] R. E. Wing, *Starch citrate: preparation and ion exchange properties*, Starch, 48 (1996), 275–279.

[7] J. R. Memon, S. Q. Memon, M. I. Bhanger, G. Z. Memon, A. El-Turki, and G. C. Allen, *Characterization of banana peel by scanning electron microscopy and FT-IR spectroscopy and its use for cadmium removal*, Colloids Surf B Biointerfaces, 66 (2008), 260–265.

[8] A. H. Al-Dujaili, A. M. Awwad, and N. M. Salem, *Biosorption of cadmium (II) onto loquat leaves (Eriobotrya japonica) and their ash from aqueous solution, equilibrium, kinetics, and thermodynamic studies*, Int J Ind Chem, 3 (2012), 22.

[9] B. Zhu, T. Fan, and D. Zhang, *Adsorption of copper ions from aqueous solution by citric acid modified soybean straw*, J Hazard Mater, 153 (2008), 300–308.

[10] J. M. J. Rani, G. Chandramohan, and S. Kumaravel, *Evaluation of antimicrobial activity of some garden plant leaves against Lactobacillus sp, Streptococcus mitis, Candida albicans and Aspergillus niger*, Afr J Basic Appl Sci, 4 (2012), 139–142.

[11] M. A. A. El-Remaily and A. M. Abu-Dief, *$CuFe_2O_4$ nanoparticles: an efficient heterogeneous magnetically separable catalyst for synthesis of some novel propynyl-1H-imidazoles derivatives*, Tetrahedron, 71 (2015), 2579–2584.

[12] A. M. Abu-Dief, I. F. Nassar, and W. H. Elsayed, *Magnetic $NiFe_2O_4$ nanoparticles: efficient, heterogeneous and reusable catalyst for synthesis of acetylferrocene chalcones and their antitumour activity*, Appl Organomet Chem, 30 (2016), 917–923.

[13] A. A. Marzouk, A. M. Abu-Dief, and A. A. Abdelhamid, *Hydrothermal preparation and characterization of $ZnFe_2O_4$ magnetic nanoparticles as an efficient heterogeneous catalyst for the synthesis of multi-substituted imidazoles and study of their anti-inflammatory activity*, Appl Organomet Chem, 32 (2018), e3794.

[14] D. H. K. Reddy, K. Seshaiah, A. V. R. Reddy, and S. M. Lee, *Optimization of Cd(II), Cu(II) and Ni(II) biosorption by chemically modified Moringa oleifera leaves powder*, Carbohydr Polym, 88 (2012), 1077–1086.

[15] O. Yavuz, Y. Altunkaynak, and F. Guzel, *Removal of copper, nickel, cobalt and manganese from aqueous solution by kaolinite*, Water Res, 37 (2003), 948–952.

[16] H. M. Abd El-Lateef, A. M. Abu-Dief, L. H. Abdel-Rahman, E. C. Sañudo, and N. Aliaga-Alcalde, *Electrochemical and theoretical quantum approaches on the inhibition of C1018 carbon steel corrosion in acidic medium containing chloride using some newly synthesized phenolic Schiff bases compounds*, J Electroanal Chem, 743 (2015), 120–133.

[17] H. M. Abd El-Lateef, A. M. Abu-Dief, and B. E. M. El-Gendy, *Investigation of adsorption and inhibition effects of some novel anil compounds towards mild steel in H_2SO_4 solution: Electrochemical and theoretical quantum studies*, J Electroanal Chem, 758 (2015), 135–147.

[18] H. M. Abd El-Lateef, A. M. Abu-Dief, and M. A. A. Mohamed, *Corrosion inhibition of carbon steel pipelines by some novel Schiff base compounds during acidizing treatment of oil wells studied by electrochemical and quantum chemical methods*, J Mol Struct, 1130 (2017), 522–542.

[19] O. Nygren and J. E. Wahlberg, *Speciation of chromium in tanned leather gloves and relapse of chromium allergy from tanned leather samples*, Analyst, 123 (1998), 935–937.

[20] W. J. Weber, *Physicochemical Processes for Water Quality Control*, Wiley Interscience, New York, 1972.

[21] B. S. Inbaraj, J. T. Chien, G. H. Ho, J. Yang, and B. H. Chen, *Equilibrium and kinetic studies on sorption of basic dyes by a natural biopolymer poly(γ-glutamic acid)*, Biochem Eng J, 31 (2006), 204–215.

[22] E. A. Abu-Gharib, R. M. EL-Khatib, L. A. E. Nassr, and A. M. Abu-Dief, *Kinetics of base hydrolysis of some chromen-2-one indicator dyes in different solvents at different temperatures*, J Korean Chem Soc, 55 (2011), 346–353.

[23] E. A. Abu-Gharib, R. M. El-Khatib, L. A. E. Nassr, and A. M. Abu-Dief, *Reactivity trends in the base hydrolysis of 6-nitro-2H-chromen-2-one and 6-nitro-2H-chromen-2-one-3-carboxylic acid in binary mixtures of water with methanol and acetone at different temperatures*, Kinetics and Catalysis, 53 (2012), 182–187.

[24] E. A. Abu-Gharib, R. M. EL-Khatib, L. A. E. Nassr, and A. M. Abu-Dief, *Kinetics, reactivity, initial-transition state analysis and thermodynamic parameters of base-catalyzed hydrolysis of coumalic acid in solvents with different polarities*, Arab J Chem, 10 (2017), S988–S995.

[25] I. N. Levine, *Physical Chemistry*, McGraw-Hill, New York, 4th ed., 1994.

[26] S. K. Lagergren, *About the theory of so-called adsorption of soluble substances*, Sven. Vetenskapsakad. Handingarl, 24 (1898), 1–39.

[27] E. A. Abu-Gharib, R. M. El-Khatib, L. A. E. Nassr, and A. M. Abu-Dief, *Kinetic study and reactivity trends of hydroxide ion attack on some chromen-2-one laser dyes in binary water-methanol and water-acetone mixtures*, Russ J Gen Chem, 84 (2014), 578–585.

[28] Y.-S. Ho and G. McKay, *The kinetics of sorption of divalent metal ions onto sphagnum moss peat*, Water Res, 34 (2000), 735–742.

[29] J. O. Babalola, N. A. A. Babarinde, O. A. Popoola, and V. O. Oninla, *Kinetic, equilibrium, and thermodynamic studies of the biosorption of Cd(II) and Pb(II) from aqueous solutions by Talinum triangulare (water leaf)*, Pac J Sci Technol, 10 (2009), 428–438.

[30] M. N. Pons, S. Le Bonte, and O. Potier, *Spectral analysis and fingerprinting for biomedia characterisation*, J Biotechnol, 113 (2004), 211–230.

[31] C. Aharoni and M. Ungarish, *Kinetics of activated chemisorption. Part 2.—Theoretical models*, J Chem Soc, Faraday Trans 1, 73 (1977), 456–464.

[32] H. Boparai, M. Joseph, and D. O'Carroll, *kinetics and thermodynamics of cadmium ion removal by adsorption onto nano zerovalent iron particles*, J Hazard Mater, 186 (2011), 458–465.

[33] Y. S. Ho, *Review of second-order models for adsorption systems*, J Hazard Mater, 136 (2006), 681–689.

[34] C. Pascoal Neto, J. Rocha, A. Gil, N. Cordeiro, A. P. Esculcas, S. Rocha, et al., *^{13}C solid-state nuclear magnetic resonance and Fourier transform infrared studies of the thermal decomposition of cork*, Solid State Nucl Magn Reson, 4 (1995), 143–151.

[35] M. Minamisawa, H. Minamisawa, S. Yoshida, and N. Takai, *Adsorption behavior of heavy metals on biomaterials*, J Agric Food Chem, 52 (2004), 5606–5611.

[36] M. Riaz, R. Nadeem, M. A. Hanif, T. M. Ansari, and K. U. Rehman, *Pb(II) biosorption from hazardous aqueous streams using Gossypium hirsutum (Cotton) waste biomass*, J Hazard Mater, 161 (2009), 88–94.

[37] Z. Aksu, *Biosorption of reactive dyes by dried activated sludge: equilibrium and kinetic modelling*, Biochem Eng J, 7 (2001), 79–84.

[38] H. N. Bhatti, R. Khalid, and M. A. Hanif, *Dynamic biosorption of Zn(II) and Cu(II) using pretreated Rosa gruss an teplitz (red rose) distillation sludge*, Chem Eng J, 148 (2009), 434–443.

[39] M. Malakootian, A. Fatehizadeh, N. Yousefi, M. Ahmadian, and M. Moosazadeh, *Fluoride removal using Regenerated Spent Bleaching Earth (RSBE) from groundwater: Case study on Kuhbonan water*, Desalination, 277 (2011), 244–249.

[40] H. N. Bhatti, A. W. Nasir, and M. A. Hanif, *Efficacy of Daucus carota L. waste biomass for the removal of chromium from aqueous solutions*, Desalination, 253 (2010), 78–87.

[41] J. N. Egila, B. E. N. Dauda, and T. Jimoh, *Biosorptive removal of cobalt (II) ions from aqueous solution by Amaranthus hydridus L. stalk wastes*, Afr J Biotechnol, 9 (2010), 8192–8198.

[42] T. Jimoh, J. Egila, B. E. Dauda, and Y. A. Iyaka, *Preconcentration and removal of heavy metal ions from aqueous solution using modified charcoal*, J Environ Chem Ecotoxicol, 3 (2011), 236–241.

[43] G. Ç. Dönmez, Z. Aksu, A. Öztürk, and T. Kutsal, *A comparative study on heavy metal biosorption characteristics of some algae*, Process Biochem, 34 (1999), 885–892.

[44] K. V. Kumar, S. Sivanesan, and V. Ramamurthi, *Adsorption of malachite green onto Pithophora sp., a fresh water algae: Equilibrium and kinetic modelling*, Process Biochem, 40 (2005), 2865–2872.

[45] X. F. Sun, S. G. Wang, X. W. Liu, W. X. Gong, N. Bao, B. Y. Gao, et al., *Biosorption of Malachite Green from aqueous solutions onto aerobic granules: Kinetic and equilibrium studies*, Bioresour Technol, 99 (2008), 3475–3483.

[46] V. K. Garg, R. Gupta, A. Bala Yadav, and R. Kumar, *Dye removal from aqueous solution by adsorption on treated sawdust*, Bioresour Technol, 89 (2003), 121–124.

[47] T. O. Owoyokun, *Biosorption of methylene blue dye aqueous solutions on Delonix regia (flamboyant tree) pod biosorbent*, Pac J Sci Technol, 10 (2009), 872–883.

[48] S. Chakraborty, S. De, S. DasGupta, and J. K. Basu, *Adsorption study for the removal of a basic dye: experimental and modeling*, Chemosphere, 58 (2005), 1079–1086.

[49] S. Larous, A.-H. Meniai, and M. B. Lehocine, *Experimental study of the removal of copper from aqueous solutions by adsorption using sawdust*, Desalination, 185 (2005), 483–490.

[50] L. H. Abdel-Rahman, B. S. F. Al-Farhan, A. M. Abu-Dief, et al., *Removal of toxic Pb(II) ions from aqueous solution by nano sized flamboyant pod (Delonix regia)*, Arch Chem Res, 1 (2016), 1–10.

[51] L. C. Juang, C. C. Wang, and C. K. Lee, *Adsorption of basic dyes onto MCM-41*, Chemosphere, 64 (2006), 1920–1928.

[52] C. K. Jain, D. C. Singhal, and M. K. Sharma, *Adsorption of zinc on bed sediment of River Hindon: adsorption models and kinetics*, J Hazard Mater, 114 (2004), 231–239.

[53] A. S. Özcan and A. Özcan, *Adsorption of acid dyes from aqueous solutions onto acid-activated bentonite*, J Colloid Interface Sci, 276 (2004), 39–46.

[54] A. K. Meena, G. K. Mishra, P. K. Rai, C. Rajagopal, and P. N. Nagar, *Removal of heavy metal ions from aqueous solutions using carbon aerogel as an adsorbent*, J Hazard Mater, 122 (2005), 161–170.

[55] L. H. Abdel-Rahman, A. M. Abu-Dief, M. A. Abd-El Sayed, and M. M. Zikry, *Nano sized Moringa oleifera an effective strategy for Pb(II) ions removal from aqueous solution*, Chem Mater Res, 8 (2016), 8–22.